

Rules for biologically-inspired adaptive network design

Atsushi Tero^{1,2}, Seiji Takagi¹, Tetsu Saigusa³,
Kentaro Ito¹, Dan P. Bebbler⁴, Mark D. Fricker⁴,
Kenji Yumiki⁵, Ryo Kobayashi^{5,6}, Toshiyuki Nakagaki^{1,6*}

¹Research Institute for Electronic Science,
Hokkaido University, Sapporo, 060-0812, Japan

²PRESTO JST, Japan

³Graduate School of Engineering,
Hokkaido University, Sapporo 060-8628, Japan

⁴Department of Plant Sciences, University of Oxford,
Oxford, OX1 3RB, UK

⁵Department of Mathematics and Life Sciences,
Hiroshima University, Higashi-Hiroshima 739-8626, Japan

⁶ JST, CREST, 5, Sanbancho, Chiyoda-ku, Tokyo, 102-0075, Japan

*To whom correspondence should be addressed; E-mail: nakagaki@es.hokudai.ac.jp

Transport networks are ubiquitous in both social and biological systems. Robust network performance involves a complex trade-off between cost, transport efficiency, and fault tolerance. Biological networks have been honed by many cycles of evolutionary selection pressure and are likely to yield reasonable solutions to such combinatorial optimization problems. Furthermore they develop without centralized control and may represent a readily scalable solution for growing networks in general. We show that the slime mold *Physarum*

polycephalum forms networks with comparable efficiency, fault-tolerance, and cost to those of real-world infrastructure networks - in this case the Tokyo rail system. The core mechanisms needed for adaptive network formation can be captured in a biologically-inspired mathematical model, that may have applicability to guide network construction in other domains.

Transport networks are a critical part of the infrastructure needed to operate a modern industrial society and facilitate efficient movement of people, resources, energy, and information. Despite their importance, most networks have emerged without clear global design principles and are constrained by the the priorities imposed at their initiation. Thus, the main motivation historically was to achieve high transport efficiency at reasonable cost, but with correspondingly less emphasis on making systems tolerant to interruption or failure. Introducing robustness inevitably requires additional redundant pathways that are not cost-effective in the short-term. In recent years, the spectacular failure of key infrastructure such as power grids (1, 2), financial systems (3, 4), airline baggage handling systems (5), or railway networks (6), and the predicted vulnerability of systems such as information (7) or supply networks (8), to attack, have highlighted the need to develop networks with greater intrinsic resilience.

Some organisms grow as an interconnected network as part of their normal foraging strategy to discover and exploit new resources (9–12). Such systems continuously adapt to their environment and have to balance the cost of producing an efficient network with the consequences of even limited failure in a competitive world. Unlike anthropogenic infrastructure systems, these biological networks have been subjected to successive rounds of evolutionary selection, and are likely to have found an appropriate balance between cost, efficiency, and resilience. Drawing inspiration from biology has led to useful approaches to problem-solving such as neural net-

works, genetic algorithms, or efficient search routines developed from ant-colony optimization (ACO) algorithms (13). We exploited the true slime mold *Physarum polycephalum* to develop a biologically-inspired model for adaptive network development.

Physarum is a large, single-celled amoeboid organism that forages for patchily-distributed food sources (FSs). The individual plasmodium initially explores with a relatively contiguous foraging margin to maximize the area searched. However, behind the margin, this is resolved into a tubular network linking the discovered FSs through direct connections, Steiner points, forming intermediate junctions to reduce the overall length of the connecting network, and additional cross-links that improve overall transport efficiency and resilience (11, 12, 14). Growth of the plasmodium is influenced by the characteristics of the substrate (15), can be constrained by physical barriers (16) or influenced by the light regime (17), facilitating experimental investigation of the rules underlying network formation. Thus for example, *Physarum* can find the shortest path through a maze (16–18) or connect different arrays of FSs in an efficient manner with low total length (TL) yet short average minimum distance (MD) between pairs of FSs, and a high degree of fault tolerance (FT) to accidental disconnection (11, 14, 19, 20). Capturing the essence of this system in simple rules might help guide development of de-centralized networks in other domains.

We observed *Physarum* connecting a template of 36 FSs that represented geographical locations of cities in the Tokyo area, and compared the result with the actual rail network in Japan. The *Physarum* plasmodium was allowed to grow from Tokyo and initially filled much of the available land-space, but then concentrated on FSs by thinning-out the network to leave a sub-set of larger, interconnecting tubes (Fig. 1). An alternative protocol in which the plasmodium was allowed to extend fully in the available space, and then the FSs were presented simultaneously, yielded similar results. To complete the network formation, any excess volume of plasmodium was allowed to accumulate on a large FS outside the arena (LFS in Fig. 2A).

A range of network solutions were apparent in replicate experiments (compare Fig. 2A with Fig. 1F), nevertheless, the topology of many *Physarum* networks bore similarity to the real rail network (Fig. 2D). Some of the differences may relate to geographical features that constrain the rail network, such as mountainous terrain or lakes. These constraints were imposed on the *Physarum* network by varying the intensity of illumination, as the plasmodium avoids bright light (17). This yielded networks (Fig. 2B,C) with greater visual congruence to the real rail network (Fig. 2D). Networks were also compared with the minimal spanning tree (MST, Fig. 2E), which is the shortest possible network connecting all the city positions, and various derivatives with increasing number of cross-links added (e.g. Fig. 2F), culminating in a fully connected Delaunay triangulation (DT), which represents the maximally connected network linking all the cities.

The performance of each network was characterized by the cost (TL), transport efficiency (MD), and robustness (FT), normalized to the corresponding value for the MST to give TL_{MST} , MD_{MST} and FT_{MST} . The TL of the Tokyo rail network was 1.8 fold greater than the MST (i.e. $TL_{MST} = \sim 1.8$), whilst the average TL_{MST} for *Physarum* was 1.75 ± 0.30 ($n = 21$). Illuminated networks gave slightly better clustering around the value for the rail network (Fig. 3A). For comparison, the Delaunay triangulation was ~ 4.6 -fold longer than the MST. Thus the cost of the solutions found by *Physarum* closely matched that of the rail network, with about 30 % of the maximum possible number of links in place. The transport performance of the two networks was also similar, with MD_{MST} of 0.85 and 0.85 ± 0.04 for the rail network and the *Physarum* networks, respectively. However the *Physarum* networks achieved this with marginally lower overall cost (Fig. 3A).

The converse was true for the fault tolerance (FT_{MST}) in which the real rail network showed marginally better resilience, close to the lowest level needed to give maximum tolerance to a single random failure. Thus, only 4 % of faults in the rail network would lead to isolation of

any part, whereas $14 \pm 4\%$ would disconnect the illuminated *Physarum* networks, and $20 \pm 13\%$ would disconnect the unconstrained *Physarum* networks. In contrast, simply adding additional links to the MST to improve network performance resulted in networks with poor fault tolerance (Fig. 3B).

The trade-off between fault tolerance and cost was captured in a single benefit-cost measure, expressed as the ratio of $FT/TL_{MST} = \alpha$. In general, the *Physarum* networks and the rail network had a benefit/cost ratio of ~ 0.5 for any given TL_{MST} (Fig. 3B). The relationship between different α values and the transport efficiency (Fig. 3C) highlighted the similarity in aggregate behaviour of the *Physarum* network when considering all three performance measures (MD_{MST} , TL_{MST} and FT_{MST}). The rail network was embedded in the cluster of results for the *Physarum* networks with a marginally higher α value for the same transport efficiency (Fig. 3C).

Overall, we conclude that the *Physarum* networks showed similar characteristics to those of the rail network in terms of their cost, transport efficiency, and fault tolerance. However, the *Physarum* networks self-organised without centralized control or explicit global information by a process of selective reinforcement of preferred routes and simultaneous removal of redundant connections.

We developed a mathematical model for adaptive network construction to emulate this behaviour based on feedback loops between the thickness of each tube and internal protoplasmic flow (14, 19–23) in which high rates of streaming stimulate an increase in tube diameter, whereas tubes tend to decline at low flow rates (24). The initial shape of plasmodium is represented by a randomly meshed lattice with a relatively fine spacing, as shown in Fig. 4 (t=0). The edges represent plasmodial tubes in which protoplasm flows, and nodes are junctions between tubes. Suppose that the pressures at nodes i and j are p_i and p_j , respectively, and that the two nodes are connected by a cylinder of length L_{ij} and radius r_{ij} . Assum-

ing flow is laminar and follows the Hagen-Poiseuille equation, the flux through the tube is $Q_{ij} = 8\pi r^4(p_i - p_j)/(\xi L_{ij}) = D_{ij}(p_i - p_j)/L_{ij}$, where ξ is the viscosity of the fluid, and $D_{ij} = 8\pi r^4/\xi$ is a measure of the conductivity of the tube. As the length L_{ij} is a constant, the behaviour of network is described by the conductivities, D_{ij} , of the edges.

At each time step, a random FS (node 1) is selected to drive flow through the network, so the flux includes a source term $\sum_j Q_{1j} = I_0$. A second random FS is chosen as a sink (node 2) with a corresponding withdrawal of I_0 such that $\sum_j Q_{2j} = -I_0$. As the amount of fluid must be conserved, the inflow and outflow at each internal node must balance so that i ($i \neq 1, 2$), $\sum_j Q_{ij} = 0$. Thus, for a given set of conductivities and selected source and sink nodes, the flux through each of the network edges can be computed.

To accommodate the adaptive behaviour of the plasmodium, the conductivity of each tube evolves according to the equation $dD_{ij}/dt = f(|Q_{ij}|) - D_{ij}$. The first term on the right hand side describes the expansion of tubes in response to the flux. The second term represents the rate of tube constriction, so that in the absence of flow the tubes will gradually disappear. The functional form $f(|Q|)$ is given by $f(|Q|) = |Q|^\gamma/(1 + |Q|^\gamma)$, that describes a sigmoidal response. A typical simulation result with $I_0 = 2$ and $\gamma = 1.8$ (Fig. 4), gave a network with similar features to those of both the *Physarum* system and the rail network (Fig. 2C and D, respectively).

In general, increasing I_0 promoted formation of alternative routes that improved performance by reducing MD_{MST} and made the network more fault tolerant, but with increased cost (Fig. 3A through C, supplementary Fig. 1I). Low values of γ also gave a greater degree of cross-linking, with an increased number of Steiner points (supplementary Fig. 2A, B). Conversely, decreasing I_0 (supplementary Fig. 1A) or increasing γ (supplementary Fig. 2I), drove the system towards a low cost minimal spanning tree (Fig. 2E), but with an inevitable decrease in resilience (Fig. 3B). The final network solution also depended slightly on the stochastic

variation assigned to the starting values of D_{ij} . Judicious selection of specific parameter combinations ($I_0 = 0.20, \gamma = 1.15$) yielded networks with remarkably similar topology and metrics to the Tokyo rail network (supplementary Fig. 2B). However, by increasing I_0 to 2 and γ to 1.8, the simulation model also achieved a benefit-cost ratio ($\alpha = \text{FT}/\text{TL}_{MST}$) that was better than those of the rail or *Physarum* networks, reaching a value of 0.7 with an almost identical transport efficiency of 0.85 (Fig. 3C). Conversely, the consequence of the increased TL_{MST} observed in the rail or *Physarum* networks would be to confer greater resilience to multiple simultaneous failures at the expense of increased cost, rather than tolerance to a single disconnection that is evaluated by FT_{MST} .

In summary, we have developed a simple, biologically-inspired mathematical model that can capture the basic dynamics of network adaptability through iteration of local rules and produces solutions with comparable or better properties than those of real-world infrastructure networks. Furthermore, the model has a number of tuneable parameters that allow adjustment of the benefit-cost ratio to increase specific features, such as fault tolerance or transport efficiency, while keeping costs low. Such a model may provide a useful starting point to improve routing protocols and topology control for self-organized networks such as remote sensor arrays, mobile ad-hoc networks or wireless mesh networks (25).

References

1. R. Albert, I. Albert, G. Nakarado, *Phys. Rev. E* **69**, 025103R (2004).
2. R. V. Solé, M. Rosas-Casals, B. Corominas-Murtra, S. Valverde, *Phys. Rev. E* **77**, 026102 (2003).
3. R. May, S. Levin, G. Sugihara, *Nature* **451**, 893 (2008).
4. J. Kambhu, S. Weidman, N. Krishnan, *Economic Policy Review* **13**, 1 (2007).

5. House of Commons - Transport Committee, *The Opening of Heathrow Terminal 5 HC 543* (The Stationery Office, 2008).
6. *Train Derailment at Hatfield* (Independent Investigation Board, Office of Rail Regulation, 2006).
7. R. Albert, H. Jeong, A.-L. Barabási, *Nature* **406**, 378 (2000).
8. R. Carvalho, *et al.*, *arXiv:0903.0195* (2009).
9. D. Bebbber, J. Hynes, P. Darrah, L. Boddy, M. Fricker, *Proc. Roy. Soc. Lond. B* **274**, 2307 (2007).
10. J. Buhl, *et al.*, *Behav. Ecol. Sociobiol.* **63**, 451 (2009).
11. T. Nakagaki, H. Yamada, M. Hara, *Biophys. Chem.* **107**, 1 (2004).
12. T. Nakagaki, R. Kobayashi, Y. Nishiura, T. Ueda, *Proc. R. Soc. Lond. B* **271**, 2305 (2004).
13. A. Colomi, *et al.*, *Int. Trans. Op. Res.* **3**, 1 (1996).
14. A. Tero, T. Nakagaki, K. Toyabe, K. Yumiki, R. Kobayashi, *Int. J. Unconventional Comp.* (2008, in press).
15. Takamatsu, A. Takaba, G. E. Takizawa, *J. Theor. Biol.* **256**, 29 (2009).
16. T. Nakagaki, H. Yamada, A. Tóth, *Nature* **407**, 470 (2000).
17. T. Nakagaki, *et al.*, *Phys. Rev. Lett.* **99**, 068104 (2007).
18. T. Nakagaki, H. Yamada, A. Tóth, *Biophys. Chem.* **92**, 47 (2001).
19. A. Tero, K. Yumiki, R. Kobayashi, T. Saigusa, T. Nakagaki, *Theory in Biosciences* **127**, 89 (2008).

20. T. Nakagaki, R. Guy, *Soft Matter* **4**, 57 (2008).
21. T. Nakagaki, T. Saigusa, A. Tero, R. Kobayashi, *Proc. Int. Symp. On Topological Aspects of Critical Systems and Networks* pp. 94–100 (2007).
22. A. Tero, R. Kobayashi, T. Nakagaki, *J. Theor. Biol.* **244**, 553 (2007).
23. A. Tero, R. Kobayashi, T. Nakagaki, *Physica A* **363**, 115 (2006).
24. T. Nakagaki, H. Yamada, T. Ueda, *Biophys. Chem.* **84**, 195 (2000).
25. I. Akyildiz, X. Wang, W. Wang, *Computer Networks* **47**, 445 (2005).
26. This work was supported MEXT KAKENHI No.18650054 and No. 20300105, Human Frontier Science Program Grant RGP51/2007. EU Framework 6 Contract No 12999 (NEST) and NERC No. A/S/882.

Figure 1: **Network formation in *Physarum polycephalum*.** (A) At $t = 0$ a small plasmodium of *Physarum* was placed at the location of Tokyo in an experimental arena bounded by the Pacific coastline (white border) and supplemented with additional food sources at each of the major cities in the region (white dots). The plasmodium grew out from the initial food source with a contiguous margin and progressively colonized each of the food sources (B-F). Behind the growing margin, the spreading mycelium resolved into a network of tubes interconnecting the food sources.

Figure 2: **Comparison of the *Physarum* networks with the Tokyo rail network.** (A) In the absence of illumination, the *Physarum* network resulted from even exploration of the available space. (B) Geographical constraints were imposed on the developing *Physarum* network using an illumination mask to restrict growth to more shaded areas corresponding to low altitude regions. The ocean and inland lakes were also given strong illumination to prevent growth. The resulting network (C) was compared with the rail network in the Tokyo area (D). The minimum spanning tree (MST) connecting the same set of city nodes is shown in (E), along with a model network constructed by adding additional links to the MST (F).

Figure 3: **Transport performance, resilience and cost for *Physarum* networks, model simulations and the real rail networks.** The transport performance of each network was measured as the minimum distance between all pairs of nodes, normalized to the MST (MD_{MST}), and plotted against the total length of the network normalized by the MST (TL_{MST}), as a measure of cost (A). Black circles and light blue squares represent results obtained from *Physarum* in the absence or presence of illumination, respectively. Crosses represent results for reference networks and the green triangle the actual rail network. Open red circles represent simulation results as I_0 was varied from 0.20 to 7.19 at a fixed $\gamma (= 1.80)$ and initial random fluctuations of D_{ij} . The fault tolerance (FT) was measured as the probability of disconnecting part of the network with failure of a single link (B), symbols as in (A). The benefit to cost ratio, $\alpha = FT/(TL_{MST})$, is shown as a series of dotted lines. The relationship between MST (MD_{MST}) and α is shown in (C). Although the overall performance of the experiment and real rail network are clustered together, the simulation model achieves better fault tolerance for the same transport efficiency.

Figure 4: **Network dynamics for the simulation model** (A)-(D) Show a typical time course for evolution of the simulation. Time is shown in arbitrary units and cities as blue dots. Each city was modeled as a single FS, apart from Tokyo which was an aggregate of seven FS to match the importance of Tokyo as the center of the region. At the start (A), the available space was populated with a finely meshed network of thin tubes. Over time, many of these tubes died out, whilst a limited number of tubes became selectively thickened to yield a stable, self-organized solution. $\gamma = 1.80$, $I_0 = 2.00$.

Supplementary Figure 1: The effect of varying I_0 on network architecture Simulation results are shown for increasing values of I_0 at a fixed value of γ (1.80). The networks increase the number of cross connections from close to a minimum spanning tree at the lowest values of I_0 (A), to give a better connectivity at higher values (I). Numbers in parenthesis are (γ , I_0 , TL_{MST} , FT_{MST} and MD_{MST}).

Supplementary Figure 2: The effect of varying γ on network architecture Simulation results are shown for increasing values of γ at a fixed value of I_0 (0.2). At the lowest value of γ , much of the original mesh remains, with little development of a preferential distribution network (A). As γ is increased, the network progressively resolves towards the minimum spanning tree (I). The parameter combinations shown in B, give a network that closely matches the Tokyo rail network and the illuminated *Physarum* networks. Numbers in parenthesis are (γ , I_0 , TL_{MST} , FT_{MST} and MD_{MST}).

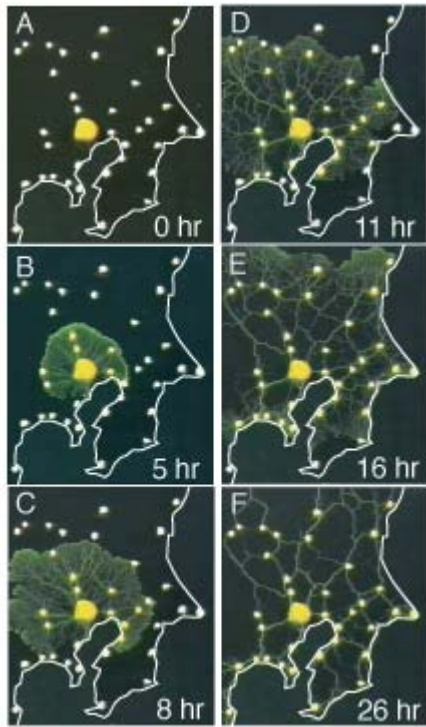


Fig. 1

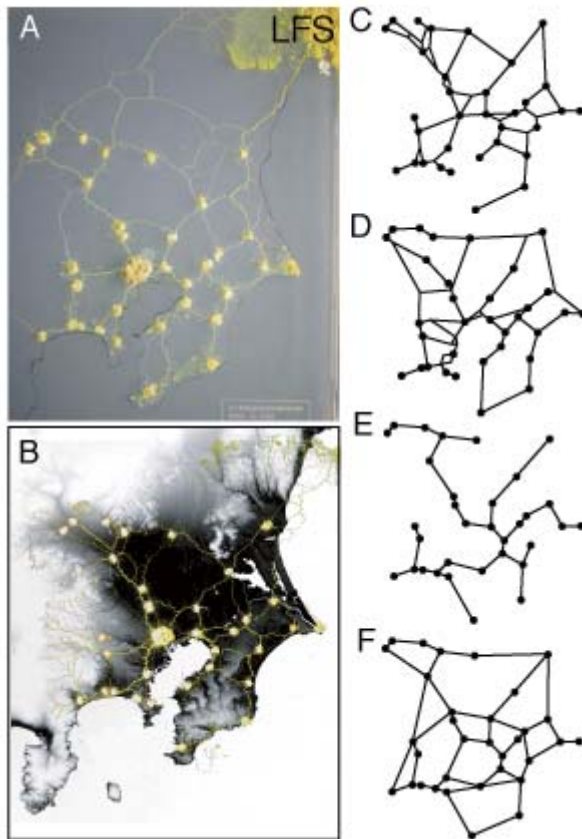


Fig. 2

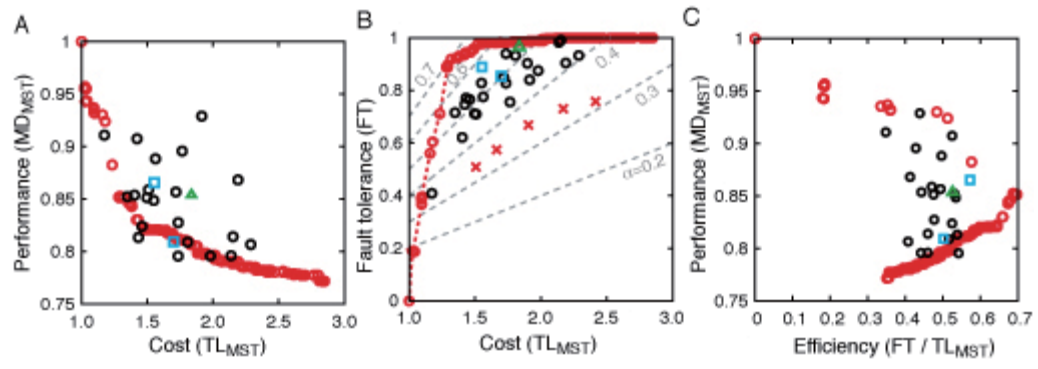


Fig. 3

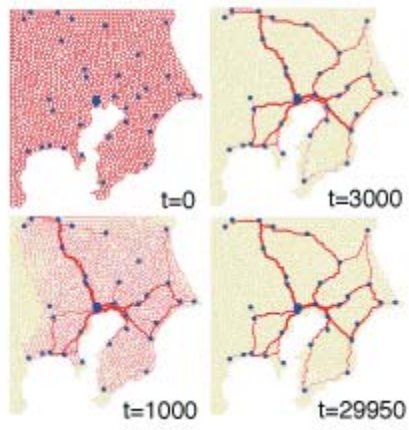


Fig.4